Library Progress International
Vol.44, No.3, Jul-Dec 2024: P. 79-89

Print version ISSN 0970 1052
Online version ISSN 2320 317X

Original Article

Available online at www.bpasjournals.com

Investigation On the Control of a DFIG And Dual-Energy Storage System for Stable Performance.

Dr. Nilaykumar A. Patel[1], Dr. Jigar Sarda[2], Khush N. Patel[3] and Keya N. Patel[4]

[1, 2, 4] Dept. of Electrical Engineering, CSPIT-CHARUSAT UNIVERSITY, Changa, Gujarat, India
[3] Schulich School of Engineering, University of Calgary, Calgary, Canada
nilaypatel.ee@charusat.ac.in
jigarsarda.ee@charusat.ac.in
Khush.patel1@ucalgary.ca
keyap675@gmail.com

How to cite this article: Nilaykumar A. Patel, Jigar Sarda, Khush N. Patel and Keya N. Patel (2024). Investigation On the Control of a DFIG And Dual-Energy Storage System for Stable Performance. 44(3), Library Progress International, 79-89

Abstract

Utilizing an energy storage system is a very efficient method to offset the fluctuations in wind power. This study suggests utilizing a hybrid storage energy system to offset the major components based on the frequency content analysis of DFIG power fluctuations. This system comprises a battery for energy storage and a super-capacitor. Subsequently, it establishes a fuzzy sliding control approach for a Dual Energy Storage System (DESS). The implementation of a fuzzy controller can effectively mitigate the undesirable phenomenon of chattering that may occur when using a sliding controller. By examining the step response of the control system under disturbance, the robustness of the fuzzy sliding controller in the wind power DESS simulation model on MATLAB is confirmed. The simulation calculation conclusively illustrates the energy storage system's output and state of charge (SOC), affirming the DESS controller's effectiveness in reducing fluctuations and improving disturbance rejection.

Keywords: fuzzy sliding; wind power; wavelet packet decomposition; energy storage; power smooth

1. Introduction

The pollutant emission from traditional power generation has a direct impact on climate, ecology, and human health. Renewable energy injected into the power grid can reduce emissions and fuel dependence [1,2] . Wind power generation has become an important part of renewable energy. However, the intermittent, volatile characteristics of wind power will integrate the randomness and insecurity of the traditional power system, making the power grid difficult to schedule, which may increase the cost of power trading and reduce power supply reliability [3,4].

Energy Storage System (ESS) has the advantages of fast response time, flexibility, and a wide range of applications, and is suitable for the whole regulation period [5]. It has no inertia effects and is environmentally friendly. Connecting an Energy Storage System to renewable energy can regulate power output and improve grid stability. At present, the research on Doubly Fed Induction Generator wind farms is mostly related to control strategies for the promotion of wind power production. The reactive power of Doubly Fed Induction Generator has rarely been applied to increase grid reactive power reserve until now. Energy storage technology can mitigate the adverse effects of wind power fluctuations on the system by controlling electricity in four quadrants [6] . Additionally, there has been a growing interest in studying DESSs that combine different types of energy storage media to take use of their complementing qualities [7].

Reference [8] employs an active parallel DESS to mitigate the tidal disturbance at the wind farm grid connection point. This is achieved by integrating batteries and super batteries to stabilize the fluctuating power of wind energy in real time. Reference [9, 10] utilizes a DESS consisting of batteries and super-capacitors to enhance the efficiency of photovoltaic power-producing systems. Reference [11] employs a DESS consisting of super-capacitors and lithium iron phosphate batteries. It utilizes the exponential smoothing method to dynamically update the overall output reference value of the

photovoltaic power station in real-time. This approach enables hierarchical control of the photovoltaic power station. In their study, researchers in Reference [12] introduced a method for mitigating wind level fluctuations. This method relies on optimizing the classification of charge states, and it involves the use of both an optimization control layer and a coordination control layer. The goal is to achieve synchronized control of the charge state of super-capacitors and battery equipment. In their study, the authors of reference [13] introduced a two-layer energy management scheme for a DESS that utilizes both batteries and super-capacitors. This scheme successfully achieved the optimization of central management by following the instructions of the dispatch center and regulating local demand. All of the aforementioned references examine the control approach of energy storage devices. The anti-interference performance of energy storage control systems is a crucial component in assessing the stability of control systems. However, research is scarce on this topic.

This paper focuses on the portion of wind power fluctuations below 1 Hz, as the portion above 1 Hz is absorbed by the inertia of the wind turbine. To mitigate the variability of wind power output, this study employs wavelet packet decomposition to categorize the wind power output into three distinct components: very low frequency (0~0.02 Hz), moderate-low frequency (0.02~0.2 Hz), and low-frequency component (0.2~1 Hz). The Technical Regulations given by Ministry of New and Renewable Energy of India for Wind Farm Access to Power Systems considers the very-low frequency component as the anticipated value for wind power grid connection. To address the moderate-low frequency and low-frequency components, a control method is suggested. This method involves utilizing a DESS consisting of batteries and super-capacitors, along with a fuzzy sliding mode controller, to achieve smoothness. An analysis is conducted on the anti-disturbance performance of the fuzzy sliding mode controller using a simulation model of a wind power DESS constructed on the MATLAB platform. This paper compares and calculates the stability of the wind farm output and the state of charge of the energy storage equipment before and after implementing the proposed control method. The aim is to verify the impact of the control method on stabilizing wind power output and enhancing the system's resistance to disturbances.

2 Doubly-fed wind power system with Dual-energy storage access

2.1 Test System

Figure 1 illustrates the configuration of a wind power system featuring a DESS connected to the low-voltage side of a doubly-fed wind farm grid connection point. The system comprises a set of n doubly-fed wind turbines. The DESS's topology employs a distributed structure, which is advantageous for the wind farm's expansion. A bidirectional DC/DC boost converter is placed between the super-capacitor energy storage system and the inverter, resulting in a reduction in the number of super-capacitors connected in series and cost savings. The bidirectional DC/DC boost converter's topology is illustrated in Figure 2. It consists of IGBTs named Q_1 and Q_2, VD_1, and VD_2 are reverse diodes, C is for voltage regulator capacitor, and a buffer energy storage inductor L.

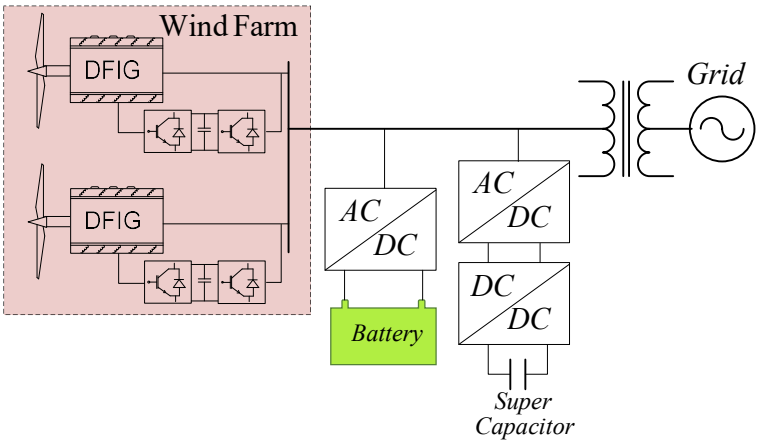

Fig. 1 DFIG system with Dual energy system

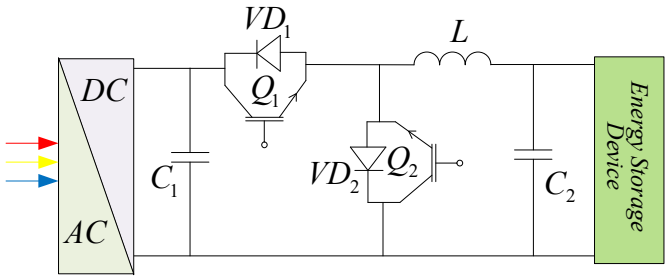

Fig. 2 Boost converter: DC/DC bidirectional

2.2 Wind power output fluctuation index

The adverse effects of wind power output variability on power system operation and dispatch primarily hinge on its maximum rate of change. The maximum change in wind power output fluctuation is equal to the absolute difference between the highest and lowest wind power outputs observed during the sampling time period of 600 minutes. The expression is

$$\Delta P(t) = \underset{t=0\to 600_{\text{minutes}}}{\text{maximum}}\left[P(t)\right] - \underset{t=0\to 600_{\text{minutes}}}{\text{minimum}}\left[P(t)\right] \quad (1)$$

Where: $\Delta P(t)$ is the maximum change of active power within the time [0, 600]. $\underset{t=0\to 600_{\text{minutes}}}{\text{maximum}}\left[P(t)\right]$ is the maximum value of active power output; $\underset{t=0\to 600_{\text{minutes}}}{\text{minimum}}\left[P(t)\right]$ is the minimum value of active power output.

This paper mainly considers the fluctuation index of wind power output power on a 1-min time scale.

2.3 Control strategy of DESS

The DESS is employed to compensate for the disparity between the actual output power P_G of the wind turbine and the desired grid-connected power value P_{ref}. This research utilizes the very low frequency component of the wind power output power after wavelet packet decomposition as the target value for grid-connected power. The battery possesses a high energy density and low power density, making it suitable for smoothing out the moderate-low frequency component. On the other hand, the super-capacitor exhibits a high power density and extended cycle life, making it ideal for smoothing out the low-frequency component [14]. Figure 3 displays the diagram of the system control block.

3 Design of DESS controller

3.1 wavelet packet based decomposition controller design

The decomposition of wind power is essentially a process of filtration. Conventional filters lack sensitivity to abrupt changes in signals with high volatility, leading to distortion in the filtered output. The wavelet transform is well-suited for analyzing mutation signals that are non-stationary [15]. Wavelet packet decomposition separates the moderate-low frequency component from the low-frequency component of the signal, allowing for precise study of the signal's time-frequency localization. The algorithm used is the wavelet packet decomposition algorithm at the first layer, as referenced by [15].

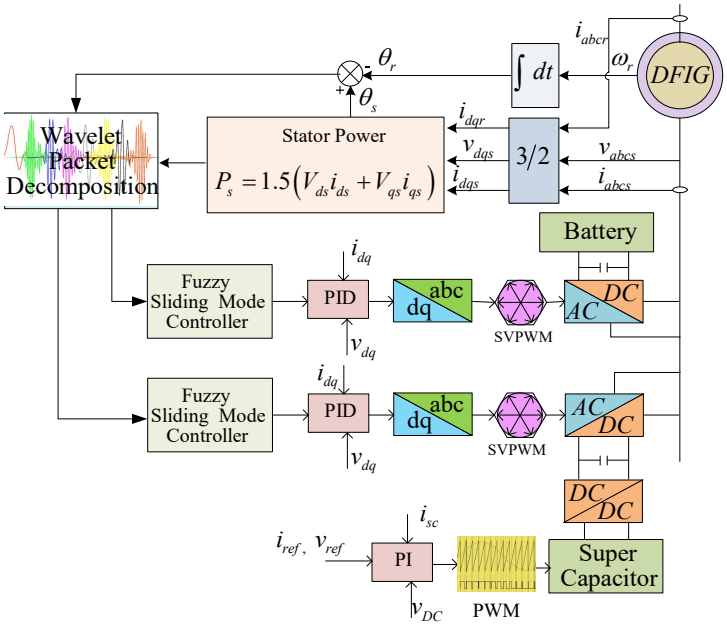

Fig. 3 Diagram of Dual-energy control system

$$\left.\begin{aligned} P_{1,0}^{n}(t) &= \sum_{k} i_{k-2l} P_G \\ P_{1,1}^{n}(t) &= \sum_{k} j_{k-2l} P_G \end{aligned}\right\} \tag{2}$$

Where: i_{k-2l} and j_{k-2l} are the low-pass and high-pass filter coefficients of wavelet packet decomposition respectively; $P_{1,0}^{n}(t)$ is the second lowest coefficient of frequency of the first layer decomposition; $P_{1,1}^{n}(t)$ is the coefficient of low frequency of the first layer decomposition. The second lowest frequency component and the low-frequency component are reconstructed using the second lowest frequency coefficient and the low-frequency coefficient. The calculating formula is as follows.

$$\left.\begin{aligned} P_{1,0}^{n}(t) &= \sum_{k}\left[n_{l-2k} P_{1,0}^{2n}(t) + m_{l-2k} P_{1,0}^{2n+1}(t)\right] \\ P_{1,1}^{n}(t) &= \sum_{k}\left[n_{l-2k} P_{1,1}^{2n}(t) + m_{l-2k} P_{1,1}^{2n+1}(t)\right] \end{aligned}\right\} \tag{3}$$

In the formula: $P_{1,0}(t)$ and $P_{1,1}(t)$ are the reconstructed moderate-low frequency component and low-frequency component respectively; n_{l-2k} and m_{l-2k} are the low-pass filter coefficient and high-pass filter coefficient of wavelet packet reconstruction respectively. Similarly, suppose the wind power output power very-low frequency component after h-layer wavelet packet decomposition is P_{ref}, the moderate-low frequency component is P_b^*, and the low-frequency component is P_{SC}^*. Its mathematical expression is

$$\left.\begin{aligned} P_{ref} &= P_{h,0}(t) \\ P_b^* &= \sum_{k=1}^{x} P_{h,k}(t) \\ P_{SC}^* &= \sum_{k=x+1}^{2^n-1} P_{h,k}(t) \end{aligned}\right\} \tag{4}$$

In the formula, m is the dividing point between the moderate-low frequency and low-frequency components.

3.2 Controller design for fuzzy sliding mode

Fuzzy control is not dependent on the exact mathematical model of the controlled object and can effectively handle the impact of nonlinear elements. It also exhibits significant resilience to variations in the parameters of the controlled item. Nevertheless, the values of the fuzzy controller's parameters must be established by iterative experimentation and cannot be reliably and fully examined. Sliding mode variable structure control is a robust control technique employed to address nonlinear control problems, particularly those arising from modeling inaccuracies [16]. Nevertheless, the variable structure control system's sliding mode is susceptible to high-frequency jitter caused by non-ideal causes including switch flipping and system failure [17]. This study integrates the merits and demerits of fuzzy control with sliding mode control to create a fuzzy sliding mode controller. The controller is then used to the DESS. Figure 4 displays the block diagram of the sliding fuzzy controller.

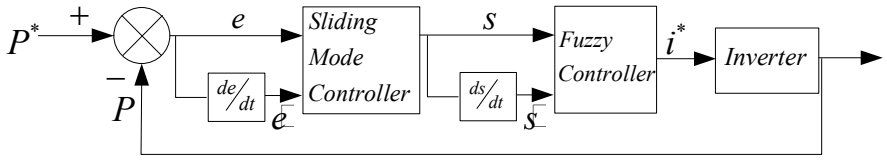

Fig. 4 Block Diagram of sliding fuzzy controller

In the figure: P^* represents the target active power output from the DESS; P represents the actual active power output from the DESS. The inputs of the sliding mode controller are the power error value and the derivative error value, and the calculation formula is:

$$e_r[t] = P_{\text{target}} - P_{\text{actual}} \tag{5}$$

$$de_r[t] = \left[e_{r(Current)} - e_{r(\text{Previous})} \right] / T_s \tag{6}$$

Where T_s is the sampling time.

The sliding mode controller switching function is…

$$s_w[t] = c * e_r[t] + de_r[t] \tag{7}$$

$$ds_w[t] = \left[s_{w(Current)} - s_{w(\text{Previous})} \right] / T_s \tag{8}$$

In the formula, c is a positive constant.

This paper adopts a two-input fuzzy controller and directly designs the target value i^* of the current loop through the control law of the fuzzy system. Two inputs namely, the switching function and its rate of change are given to the fuzzy system, and the output of the system is the change in the current Δi. Finally, the proportionate switching control function is utilized to calculate the target value i^*. The calculation formula is:

$$i^*(t) = \left(\alpha * |e| + \beta * \dot{e} \right) \text{sgn}(s) + \Delta i \tag{9}$$

Where α and β are constants greater than zero.

The fuzzy set defined in this paper is

$$s = \dot{s} = \Delta i = \{BN, AN, TN, N, TP, AP, BP\}$$

Where BN is big negative, AN is average negative, TN is tiny negative, N is null, BP is big positive, AP is average positive, TP is tiny positive.

The territory is defined as [-3, 3], and the fuzzy variables use triangular membership functions and Gaussian membership functions. The membership functions are shown in Figures 5 and 6.

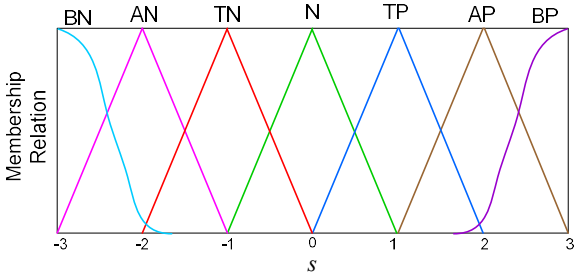

Fig. 5 Fuzzy Control Membership function for switching

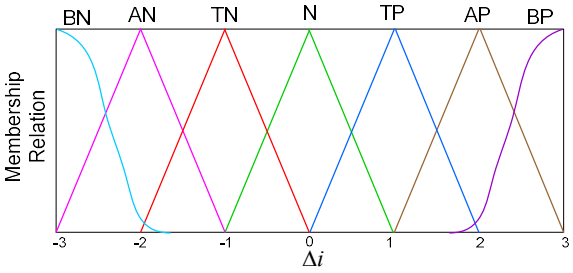

Fig. 6 Fuzzy Control Membership function for Δi

The control strategy of the fuzzy controller is as follows:

(1) When s and $\dot{s}$ are both positive, the stable point of the sliding mode system has not been reached. It is necessary to control the input to a maximum value Δi to reduce $s\dot{s}$ rapidly.

(2) When s and $\dot{s}$ are of different signs, the predominant condition of $s\dot{s} < 0$ is satisfied. It is not necessary to adjust the control quantity so that the control quantity Δi output is zero.

(3) When s and $\dot{s}$ are both negative, $s\dot{s}$ is positive, and it is necessary to adjust the control quantity to a minimum to reduce $s\dot{s}$ rapidly.

The control rules of the output function are shown in Table 1.

Table 1 Control rule of output Δi

$\dot{s}$ / s	BN	AN	TN	N	TP	AP	BP
BP	N	TP	AP	BP	BP	BP	BP
AP	TN	N	TP	AP	BP	BP	BP
TP	AN	TN	N	TP	AP	BP	BP
N	BN	AN	TN	N	TP	AP	BP
TN	BN	BN	AN	TN	N	TP	AP
AN	BN	BN	BN	AN	TN	N	TP
BN	BN	BN	BN	BN	AN	TN	N

4 Case Analysis

4.1 Verification of fuzzy sliding mode controller

Figure 7 displays the response curve obtained by comparing the unit step response of the fuzzy sliding mode controller and the standard PID regulator while applying a disturbance signal at 0.5 s. The fuzzy sliding mode control system exhibits

reduced overshoot, rapid recovery after disturbance, and superior anti-interference performance compared to the standard PID control system.

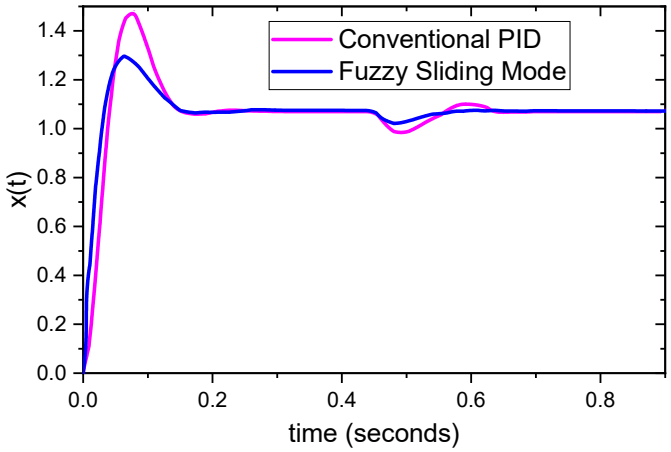

Fig. 7 Fuzzy sliding and PID system response comparison

4.2 Verification of wind power DESS

To simplify the complexity of the wind power generation system, this paper adopts 40 no. of 0.6MW doubly fed wind turbines equivalent to the wind power generation system, and the simulation system sampling time T_s is 10^{-5} s. The rated voltage of the converter DC side is 1200 V, the converter DC side capacitance is 0.01 F, the wind turbine grid voltage is 690 V, and the system frequency is 50 Hz. The parameters of the energy storage equipment are shown in Table 2.

Table 2 Performance of energy storage device

Device name	Capacity
Battery	7.5 MWh
Super Capacitor	3.0 MWh

The frequency of the power switch device IGBT is 2850 Hz, the inductance of the bidirectional DC/DC converter of the super-capacitor energy storage system is 6 mH, and the boost capacitor is 0.095 F. The wind power operation time is 600 min, and the dual energy storage takes into account the 1 min evaluation index to smooth the fluctuation of wind power output power. The wind power output power curve is shown in Figure 8.

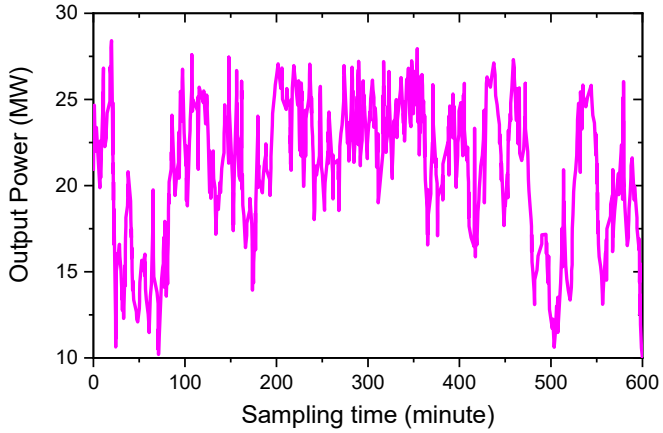

Fig. 8 Curve of wind output power

This study utilizes the db9 wavelet packet to conduct a 5-layer decomposition of the wind farm output. The outcome of the decomposition is presented in Figure 9. This research focuses exclusively on frequency fluctuations below 1 Hz, as any fluctuations beyond this threshold are effectively absorbed by the inertia of the wind turbine. Using spectrum analysis, the very low frequency component has a frequency range of 0~0.02 Hz, the moderate-low frequency component has a frequency range of 0.02~0.2 Hz and the low frequency component has a frequency range of 0.2~1 Hz. Figure 9 demonstrates that the curve of the very low frequency component is notably smooth, making it suitable as the desired

value for wind power grid-connected electricity. The charging and discharging of batteries and super-capacitors are targeted at the moderate-low frequency component and low frequency component, respectively, based on their complementing features. The moderate-low frequency component has an amplitude range of -5 to 5 MW, whereas the low-frequency component has an amplitude range of -4.5 to 4.5 MW.

Figure 10 illustrates the contrast between the grid-connected power of wind power following the implementation of a DESS and the grid-connected power without such a system. As per the Indian standard, this paper establishes a limit of 3 MW for the variation of wind power output. Figure 11 illustrates the comparison of wind power grid-connected electricity before and after the implementation of the DESS. The DESS compensates for the wind power grid-connected power with a maximum change of 0 to 1.02 MW. Meeting the wind power grid-connected requirement effectively smooths the electricity generated from wind and improves the efficiency of wind energy use. Figure 12 depicts the wind power output that is absorbed and adjusted by the battery and super-capacitor when they are being charged and discharged. The figure demonstrates that the super-capacitor and the battery effectively smooth out the low-frequency and moderate-low-frequency components of the wind power output fluctuation derived from wavelet packet decomposition. Furthermore, due to the rapid charging and discharging properties of super-capacitors, it is possible to prevent the need for frequent charging and discharging of batteries. Simultaneously, the ample battery capacity significantly decreases the entire equipment building expenses, satisfying both the response time demands and achieving cost-effectiveness in terms of lifespan and expenses.

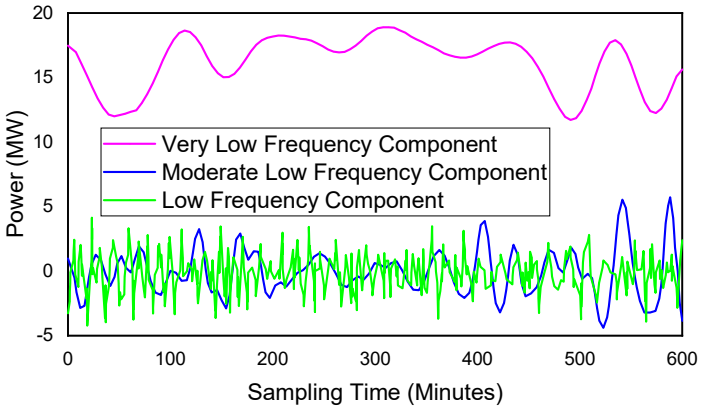

Fig. 9 Diagram of wind output power by wavelet packet

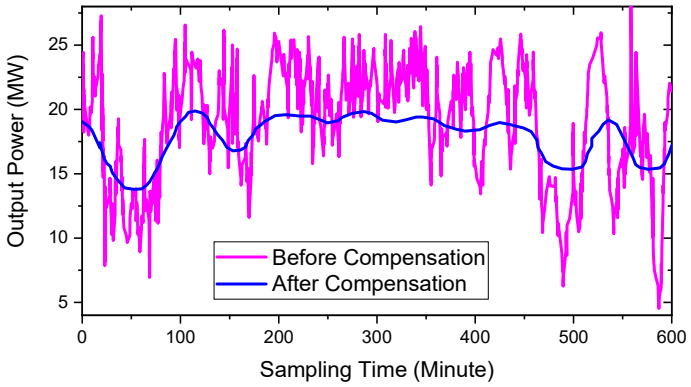

Fig. 10 DFIG output power

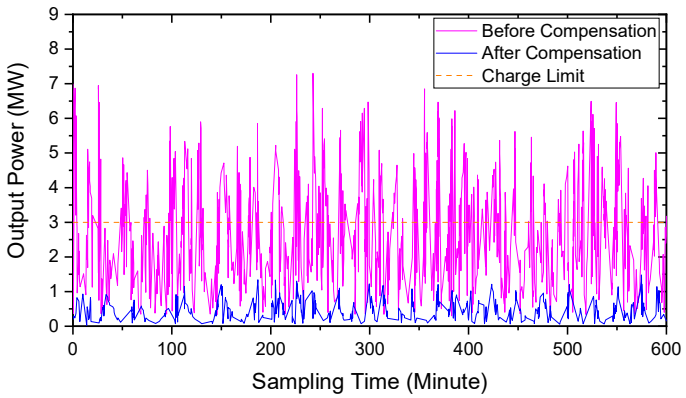

Fig. 11 DFIG power variation before and after compensation

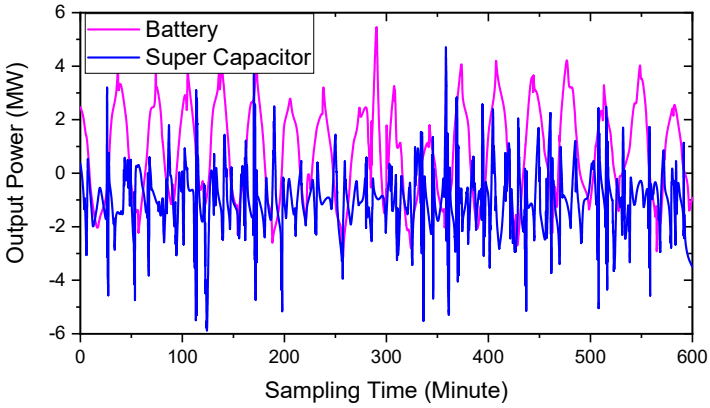

Fig. 12 Battery and super-capacitor power

The level of charge is a crucial criterion for determining whether the energy storage device is operating abnormally due to excessive charging or discharging. By continuously monitoring the level of charge in the energy storage device, it is possible to accurately determine the current remaining capacity of the device in real time. To guarantee the secure and consistent functioning of the system within the sequential arrangement of each energy storage unit, it is imperative to enhance the voltage equilibrium safeguard and state of charge safeguard of the energy storage unit. This work specifically examines the optimal range for the state of charge of the energy storage device, and establishes the initial state of charge for the DESS as 0.5. Figure 13 displays the state of charge curves of the battery and super-capacitor in response to the wind power output. The dashed line represents the battery, while the continuous line represents the super-capacitor.

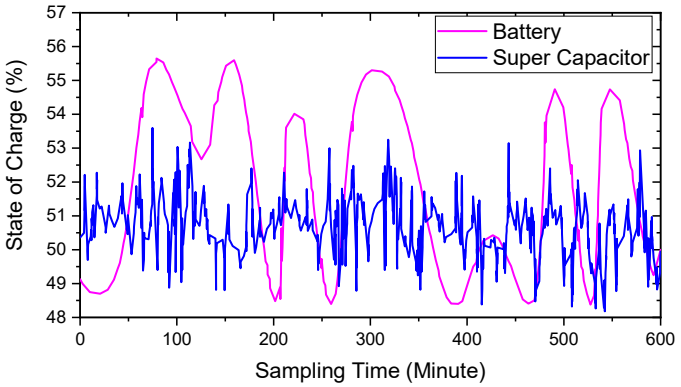

Fig. 13 SOC of DESS

As shown in Figure 13, the charge state of the super-capacitor and energy storage battery varies from 46.5% to 57% and 46%~53.8% respectively in response to wind power output, that is, they are both within the safe range, and there is no overcharge or over-discharge. Compared with Figure 12, the charged state of the battery and super-capacitor is consistent with the output of active power. The DESS gives full play to the characteristics of small capacity and fast charge and discharge of super-capacitors, making up for the shortcomings of slow charging and discharging of single battery energy

storage and frequent charge and discharge that reduces service life, which improves the response speed of the energy storage system and also improves the anti-interference ability of the system.

5 Conclusion

This paper chooses a DESS consisting of batteries and super-capacitors to reduce the fluctuation in power output of the doubly fed wind power generation system, based on an analysis of wind power output characteristics. Additionally, a fuzzy sliding mode control strategy for the system is proposed. By examining the unit-step response of the control system, we can confirm the effectiveness of the control strategy in mitigating disturbances. Additionally, by analyzing the power at the grid connection point after compensation by the DESS and the charge status of the DESS, we can demonstrate the efficacy of the control strategy.

References:

[1] Bhatt, P., Long, C., Mehta, B. and Patel, N., "Optimal utilization of reactive power capability of renewable energy based distributed generation for improved performance of distribution network", Renewable Energy and Climate Change: Proceedings of REC 2019, Springer Singapore, pp. 141-152. 2020. doi:10.1007/978-981-32-9578-0_13.

[2] Nilaykumar Patel, Khush Patel, and Keya N. Patel, "Analysis and Mitigation of SSR in a Doubly Fed Induction Generator (DFIG) Based Wind Farm by Employing a STATCOM Controller", *Journal of Electrical Systems (JES),* vol. 20, no. 9s, pp. 2379-2384, June 2024. DOI https://doi.org/10.52783/jes.4898

[3] Jain, T. and Verma, K., "Reliability based computational model for stochastic unit commitment of a bulk power system integrated with volatile wind power", *Reliability Engineering & System Safety,* 244, p.109949. 2024

[4] Mohandes B, El Moursi MS, Hatziargyriou N, El Khatib S., "A review of power system flexibility with high penetration of renewables", *IEEE Transactions on Power Systems*. Vol. 34, no. 4, pp. 3140-55, February 2019

[5] Akram, U., Nadarajah, M., Shah, R. and Milano, F., "A review on rapid responsive energy storage technologies for frequency regulation in modern power systems", *Renewable and Sustainable Energy Reviews,* vol. 120, p.109626, 2020.

[6] Ayodele, T.R. and Ogunjuyigbe, A.S.O., "Mitigation of wind power intermittency: Storage technology approach", *Renewable and Sustainable Energy Reviews*, vol. *44*, pp.447-456, 2015

[7] Tan, K.M., Babu, T.S., Ramachandaramurthy, V.K., Kasinathan, P., Solanki, S.G. and Raveendran, S.K., "Empowering smart grid: A comprehensive review of energy storage technology and application with renewable energy integration", *Journal of Energy Storage*, vil. 39, p.102591, 2021.

[8] Gwabavu, M. and Raji, A., "Dynamic control of integrated wind farm battery energy storage systems for grid connection", *Sustainability*, vol. 13, no. 6, p.3112, 2021.

[9] Sodagudi, S., Manjula, C., Vinmathi, M.S., Shekhar, R., Arias Gonzáles, J.L., Ramesh Kumar, C., Dhiman, G. and Murali Dharan, A.R., "Renewable energy based smart grid construction using hybrid design in control system with enhancing of energy efficiency of electronic converters for power electronic in electric vehicles", *International Transactions on Electrical Energy Systems,* vol. 2022, no. 1, p.2986605, 2022.

[10] Kyriakopoulos, G.L. and Arabatzis, G., "Electrical energy storage systems in electricity generation: Energy policies, innovative technologies, and regulatory regimes", *Renewable and Sustainable Energy Reviews*, vol. *56*, pp.1044-1067, 2016.

[11] Pai, F.S., Huang, S.J., Ku, C.W., Chen, Y.R., Huang, B.G. and Lin, Y.C., "Voltage equalization of lithium iron phosphate batteries cooperating with supercapacitors", *IEEE International Symposium on Circuits and Systems (ISCAS),* pp. 618-621. IEEE, June 2014.

[12] Jiang, Q. and Wang, H., "Two-time-scale coordination control for a battery energy storage system to mitigate wind power fluctuations", *IEEE Transactions on Energy Conversion*, vol. 28, no. 1, pp.52-61, 2012.

[13] Liu, X., Zhao, T., Deng, H., Wang, P., Liu, J. and Blaabjerg, F., "Microgrid energy management with energy storage systems: A review", *CSEE Journal of Power and Energy Systems*, vol. 9, no. 2, pp.483-504, 2022.

[14] Khalid, M., "A review on the selected applications of battery-supercapacitor hybrid energy storage systems for microgrids", *Energies*, vol. 12, no. 23, pp.4559, 2019.

[15] Liu, H., Mi, X. and Li, Y., "Smart deep learning based wind speed prediction model using wavelet packet decomposition, convolutional neural network and convolutional long short term memory network", *Energy Conversion and Management*, vol. *166*, pp.120-131, 2018

[16] Incremona, G.P., Rubagotti, M. and Ferrara, A., "Sliding mode control of constrained nonlinear systems", *IEEE Transactions on Automatic Control*, vol. 62, no. 6, pp.2965-2972, 2016.

[17] Tasiu, I.A., Liu, Z., Wu, S., Yu, W., Al-Barashi, M. and Ojo, J.O., "Review of recent control strategies for the traction converters in high-speed train", *IEEE Transactions on Transportation Electrification*, vol. 8, no. 2, pp.2311-2333, 2022.